# Chalcogen Diimides: Relative Stabilities of Monomeric and Dimeric Structures, $[E(NMe)_2]_n$ (E = S, Se, Te; $n$ = 1, 2)

**Nicole Sandblom, Tom Ziegler,* and Tristram Chivers*,†**

Department of Chemistry, The University of Calgary, Calgary, Alberta, Canada T2N 1N4

*Received June 4, 1997*

Density functional theory (DFT) calculations have been used to investigate the process of dimerization for the three chalcogen diimides MeN═E═NMe (E = S, Se, Te). DFT calculations for these monomers reveal that the energies of the *syn*,*syn* and *syn*, *anti* isomers differ by <3.5 kJ mol$^{-1}$ for all three chalcogens while the *anti*,*anti* isomers are substantially higher in energy (by 25−39 kJ mol$^{-1}$). A qualitative understanding of this difference can be derived from consideration of the electronic structures of the chalcogen diimides. In particular, the antibonding interaction between the in-plane nitrogen lone pairs and the $p_z$ orbital on sulfur destabilizes the most sterically favorable *anti*,*anti* isomer. The calculated dimerization energies for MeN═E═NMe show that the process is endothermic ($\Delta E$ = 34.9 kJ mol$^{-1}$) for E = S, approximately thermoneutral ($\Delta E$ = −2.8 kJ mol$^{-1}$) for E = Se, and strongly exothermic ($\Delta E$ = −82.9 kJ mol$^{-1}$) for E = Te. A qualitative analysis of the orbital interactions involved in the dimerization process reveals that the LUMOs of the diimide monomers are populated in a stabilized bonding LUMO−LUMO interaction that is lower in energy than the antibonding HOMO−HOMO interaction. The most significant contribution to the energy of dimerization is the energy required to distort the planar diimide monomer into half of the butterfly dimer.

## Introduction

Since their discovery in 1956,[1] sulfur diimides RN═S═NR have been studied extensively both as ligands in transition metal complexes[2] and as reagents in organic synthesis.[3] Three geometrical isomers, *syn*,*syn* (**1**, E = S) *syn*, *anti* (**2**, E = S), and *anti*,*anti* (**3**, E = S), are possible, and their relative importance has been investigated by a variety of experimental and theoretical methods. An early VT NMR study indicated

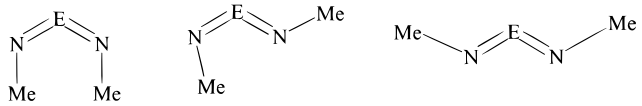


that the *syn*, *anti* isomer is the most stable in solution for R = Me,[t] Bu.[4] Subsequent multinuclear NMR studies of some bulky aryl derivatives led to the proposed presence of minor amounts of the *anti*,*anti* isomer in equilibrium with the predominant *syn*, *anti* form.[5] By contrast, the symmetrical isomer observed in solution by NMR for a variety of aryl derivatives (e.g., R = 2,4,6-$Br_3C_6H_2$, 2,6-$Me_2C_6H_3$, $C_6F_5$) was recently identified as the *syn*,*syn* isomer.[6] Consistently, both *syn*, *anti* (R = Ph,[7] 4-$C_6H_5C_6H_4$,[8] 2,4,6-$Br_3C_6H_2$[6a]) and *syn*,*syn* conformations (R = 4-$XC_6H_4S$ (X = H,[9] Cl[10]), 2,6-$Me_2C_6H_4$,[6a] $C_6F_5$[6b]) have been identified by solid-state X-ray structural determinations. Electron diffraction studies have revealed both *syn*, *anti* (R = Me)[11] and *syn*,*syn* (R = $SiMe_3$)[12] conformations in the gas phase. Thus the experimental investigations of sulfur diimides in solution, as well as in the solid state or gas phase, indicate that the *syn*,*syn* and *syn*, *anti* isomers have similar energies whose relative importance is determined by subtle substituent effects. Theoretical calculations reinforce this conclusion. *Ab initio* MO calculations (with electron correlation) indicate the *syn*,*syn* isomer to be the most stable for the parent diimide (R = H) whereas the *syn*, *anti* isomer is lowest in energy for the dimethyl derivative.[13] Recent PM3 calculations confirm the closeness in energy of these two isomeric forms and indicate, as did the earlier study,[13] that the *anti*,*anti* isomer is of substantially higher energy (by 31−38 kJ mol$^{-1}$).[6] The preference for the *syn*,*syn* geometry in certain cases has been attributed to hyperconjugation (R = $SiMe_3$)[14] or $\eta_N$,$\pi$ interactions for aryl derivatives. Dimeric structures have not been observed for sulfur diimides, but a [2+2] cycloaddition process has been invoked to explain

† Tel: 403-220-5741. Fax: 403-289-9488. E-mail: chivers@acs.ucalgary.ca.

(1) Goehring, W.; Weis, G. *Angew. Chem., Int. Ed. Engl.* **1956**, *68*, 687.
(2) (a) Vrieze, K.; van Koten, G. *Recl. Trav. Chim. Pays-Bas* **1980**, *99*, 145. (b) Chivers, T.; Hilts, R. W. *Coord. Chem. Rev.* **1994**, *137*, 201. (c) Hill, A. *Organomet. Chem. Rev.* **1994**, *36*, 159.
(3) Bussas, R.; Kresze, G.; Münsterer, H.; Schwöbel, A. *Sulphur Rep.* **1983**, *2*, 215.
(4) Grunwell, J. R.; Hoyng, C. F.; Rieck, J. A. *Tetrahedron Lett.* **1973**, *26*, 2421.
(5) (a) Kuyper, J.; Vrieze, K. *J. Organomet. Chem.* **1974**, *74*, 289. (b) Kuyper, J.; Vrieze, K. *J. Organomet. Chem.* **1975**, *86*, 127. (c) Sicinska, W.; Stefaniak, L.; Witanowski, M.; Webb, G. A. *J. Mol. Struct.* **1987**, *158*, 57.
(6) (a) Bagryanskaya, I. Yu; Gatilov, Y. V.; Shakirov, M. M.; Zibarev, A. V. *Mendeleev. Commun.* **1994**, 136. (b) Bagryanskaya, I. Yu; Gatilov, Y. V.; Shakirov, M. M.; Zibarev, A. V. *Mendeleev Commun.* **1994**, 167.
(7) Leandri, G.; Busetti, V.; Valle, G.; Mammi, M. *Chem. Commun.* **1970**, 413.
(8) Busetti, V. *Acta Crystallogr., Sect. B*, **1982**, *38*, 665.
(9) Leitch, J.; Nyburg, S. C.; Armitage, D. A.; Clark, M. J. *J. Cryst. Mol. Struct.* **1973**, *3*, 337.
(10) Olsen, F. P.; Barrick, J. C. *Inorg. Chem.* **1973**, *12*, 1353.
(11) Kuyper, J.; Isselmann, P. H.; Mijlhoff, F. C.; Spelbos, A.; Renes, G. *J. Mol. Struct.* **1975**, *29*, 247.
(12) Anderson, D. G.; Robertson, H. E.; Rankin, D. W. H.; Woollins, J. D. *J. Chem. Soc., Dalton Trans.* **1989**, 859.
(13) Raghavachari, K.; Haddon, R. C. *J. Phys. Chem.* **1983**, *87*, 1308.
(14) Rzepa, H. S.; Woollins, J. D. *J. Chem. Soc., Dalton Trans.* **1988**, 3051.

S0020-1669(97)00680-0 CCC: $15.00 
Published on Web 01/01/1998

the facile exchange of R and R′ groups for unsymmetrical derivatives RN═S═NR′ in the presence of nucleophiles.[15]

Although selenium diimides RN═Se═NR have been known for more than 20 years,[16] they are thermally unstable and no solid-state structures have been determined.[17] However, $^1$H and $^{13}$C NMR spectra are consistent with the *syn*, *anti* conformation in solution at room temperature for R = $^t$Bu.[18] Recently, the first tellurium diimides were prepared and structurally characterized.[19] They form thermally stable dimers RNTe($\mu$-N-$^t$Bu)$_2$TeN$^t$Bu (R = $PPh_2NSiMe_3$,[19a] $^t$Bu[19b]) both in the solid state (X-ray structures) and in solution (NMR studies).

Density functional theory (DFT) calculations have been applied successfully to a number of problems in chalcogen−nitrogen chemistry.[20] The purpose of this investigation is to use DFT calculations to explain the stabilization of tellurium diimides by dimerization in view of the monomeric structures of both sulfur and selenium diimides. To this end, it was also necessary to determine the relative stabilities and electronic structures of the monomers **1**−**3** for all the chalcogens.

## Computational Details

All calculations were based on approximate density functional theory within the local density approximation,[21] LDA, in the parametrization by Vosko *et al.*[22] In addition, we used Becke's[23] nonlocal exchange correction as well as inhomogenous gradient corrections for correlation due to Perdew,[24] NL-SCF. The reported calculations were performed by utilizing the vectorized version of the ADF program system developed by Baerends *et al.*[25,26] and vectorized by Ravenek.[27] The numerical integration procedure applied for the calculations was developed by te Velde.[28] The *syn*,*syn* and *anti*,*anti* monomers and the dimers were optimized with $C_{2v}$ symmetry, and the *syn*,*anti* monomer was optimized with $C_s$ symmetry. The geometry optimization procedure was based on the method developed by Versluis and Ziegler.[29] A double-$\zeta$ STO basis set[29] was employed for the *n*s and *n*p shells of the main group elements. The basis set was augmented by a single *3*d STO function except for hydrogen, where a 2p STO was used as polarization. Electrons in lower shells were considered as core and treated according to the procedure due to Baerends *et al.*[30] An auxiliary[31] set of s, p, d, f, and g STO functions, centered on all nuclei, was used in order to fit the molecular density and present Coulomb and exchange potentials accurately in each SCF cycle. All structures were optimized at the LDA level of theory. The calculated bond energies include nonlocal corrections evaluated from LDA densities.

**Table 1.** Relative Energies[a] of E(NMe)$_2$ (E = S, Se, Te) Isomers (kJ mol$^{-1}$)

| E | **1**(*syn*,*syn*) | **2**(*syn*,*anti*) | **3**(*anti*,*anti*) |
|---|---|---|---|
| S | 0.0 | 2.35 | 39.03 |
| Se | 3.35 | 0.0 | 33.79 |
| Te | 1.24 | 0.0 | 25.43 |

[a] Energies are relative to the most stable conformer.

**Table 2.** Optimized Structures of the Three E(NMe)$_2$ (E = S, Se, Te) Isomers

| isomer | bond lengths (Å)/bond angles (deg) | S | Se | Te |
|---|---|---|---|---|
| *syn*,*syn* | *d*(S═N) | 1.567[a] | 1.767 | 1.979 |
| | *d*(N−C) | 1.436 | 1.439 | 1.439 |
| | ∠NEN | 126.3[a] | 123.2 | 118.8 |
| | ∠ENC | 126.5[a] | 122.5 | 122.3 |
| *syn*,*anti* | \|*d*(S═N)\| | 1.576 (1.532)[b] | 1.779 | 1.991 |
| | \|*d*(N−C)\| | 1.437 (1.464)[b] | 1.433 | 1.427 |
| | ∠NEN | 111.9 (113.6)[b] | 103.4 | 95.3 |
| | \|∠ENC\| | 116.2 (120.4)[b] | 113.3 | 109.1 |
| *anti*,*anti* | *d*(S═N) | 1.572 | 1.774 | 1.981 |
| | *d*(N−C) | 1.444 | 1.443 | 1.434 |
| | ∠NEN | 109.1 | 102.1 | 94.2 |
| | ∠ENC | 113.6 | 112.4 | 118.4 |

[a] The corresponding values for **1** (E = S, R = $SiMe_3$) are *d*(S═N) = 1.536(3) Å, ∠NSN = 129.5(16)°, and ∠SNC = 132.9(7)°.[12] [b] Experimental data from ref 11.

## Results and Discussion

**Relative Stabilities of the Geometrical Isomers 1−3 (R = Me; E = S, Se, Te).** To determine the geometry of lowest energy, we optimized the structures of the three isomers of *N*,*N*′-dimethylchalcogen diimides: *syn*,*syn* (**1**, R = Me), *syn*, *anti* (**2**, R = Me), and *anti*,*anti* (**3**, R = Me). The calculated relative energies (see Table 1) show that conformation **1** is lowest in energy for sulfur, while **2** is the most stable isomer for both selenium and tellurium. For all three chalcogens, structures **1** and **2** are close in energy, whereas **3** on the average is 33 kJ mol$^{-1}$ less stable than the ground-state conformations. It is clear that electronic factors must dictate the relative stability of the three isomers since the least stable *anti*,*anti* (**3**) conformer would be favored by steric factors.

Table 2 lists the calculated bond lengths and bond angles for **1**−**3** (R = Me). The bond angles ∠NEN and ∠CNE increase on going from the sterically least congested isomer, *anti*,*anti* (**3**), to the most crowded isomer, *syn*,*syn* (**1**). Both angular increases will help to reduce the increasing repulsion between the two NMe fragments. The optimized structure for MeN═S═NMe in the *syn*, *anti* (**2**) conformation is in reasonable agreement with experimental values (see Table 2).[11] The calculated N═S and N−C distances differ by about 0.03 Å from


(15) Bestari, K.; Oakley, R. T.; Cordes, A. W. *Can. J. Chem.* **1991**, *69*, 94.
(16) Sharpless, K. B.; Hori, T.; Truesdale, L. K.; Dietrich, C. O. *J. Am. Chem. Soc.* **1976**, *98*, 269.
(17) In the adduct $SnCl_4$($^t$BuN═Se═N$^t$Bu) an *anti*,*anti* conformation is enforced by N,N′-chelation of the ligand to the tin center. Roesky, H. W.; Weber, K. L.; Seseke, U.; Pinkert, W.; Noltemeyer, M.; Clegg, W.; Sheldrick, G. M. *J. Chem. Soc, Dalton Trans.* **1985**, 565.
(18) Wrackmeyer, B.; Distler, B.; Gerstmann, S.; Herberhold, M. *Z. Naturforsch., B* **1993**, *48B*, 1307.
(19) (a) Chivers, T.; Gao, X.; Parvez, M. *J. Chem. Soc., Chem. Commun.* **1994**, 2149. (b) Chivers, T.; Gao, X.; Parvez, M. *J. Am. Chem. Soc.* **1995**, *117*, 2359. (c) Chivers, T.; Gao, X.; Parvez, M. *Inorg. Chem.* **1996**, *35*, 9.
(20) (a) Chivers, T.; Parvez, M.; Vargas-Baca, I.; Ziegler, T.; Zoricak, P. *Inorg. Chem.* **1997**, *36*, 1669. (b) Chivers, T.; Krouse, I.; Parvez, M.; Vargas-Baca, I.; Ziegler, T.; Zoricak, P. *Inorg. Chem.* **1996**, *35*, 5836. (c) Chivers, T.; McGarvey, B.; Parvez, M.; Vargas-Baca, I.; Ziegler, T.; *Inorg. Chem.* **1996**, *35*, 3839.
(21) (a) Gunnarsson, O.; Lindquist, I. *Phys. Rev.* **1974**, *B10*, 1319. (b) Gunnarsson, O.; Lindquist, I. *Phys. Rev.* **1976**, *B13*, 4274. (c) Gunnarsson, O.; Johnson, M.; Lindquist, I. *Phys. Rev.* **1979**, *B20*, 3136.
(22) Vosko, S. H.; Wilk, L.; Nusair, M. *Can. J. Phys.* **1990**, *58*, 1200.
(23) Becke, A. D. *J. Phys. Rev.* **1988**, *A38*, 2938.
(24) (a) Perdew, J. P. *Phys. Rev.* **1986**, *B33*, 8822. (b) Perdew, J. P. *Phys. Rev.* **1986**, *B34*, 7406.
(25) Baerends, E. J.; Ellis, D. E.; Ros, P. *Chem Phys.* **1973**, *2*, 41.
(26) Baerends, E. J. Ph.D. Thesis, Frije Universiteit, Amsterdam, 1975.
(27) Ravenek, W. In *Algorithms and Applications on Vector and Parallel Computers*; Riele, H. J. J., Dekker, Th. J., van de Horst, H. A., Eds.; Elsevier: Amsterdam, 1987.
(28) (a) Boerrigter, P. M.; te Velde, G.; Baerends, E. J. *Int. J. Quantum Chem.* **1988**, *33*, 87. (b) te Velde, G.; Baerends, E. J. *J. Comput. Chem.* **1992**, *99*, 84.
(29) Versluis, L.; Ziegler, T. *J. Chem. Phys.* **1988**, *88*, 322.
(30) (a) Snijders, J. G.; Baerends, E. J.; Vernoijs, P. *At. Nucl. Data Tables* **1982**, *26*, 483. (b) Vernoijs, P.; Snijders, J. G.; Baerends, E. J. *Slater Type Basis Functions for the Whole Periodic System*; Internal Report; Frije Universiteit: Amsterdam, 1981.
(31) Krijn, J.; Baerends, E. J. *Fitfunctions in the HFS Method*; Internal Report; Frije Universiteit: Amsterdam, 1984.

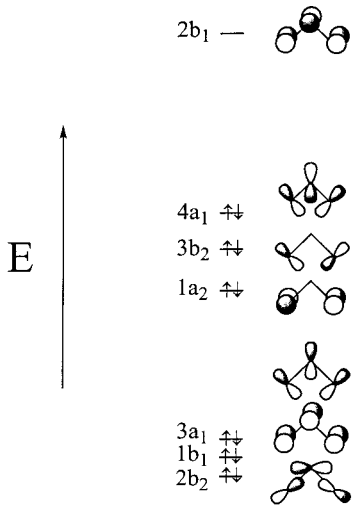


**Figure 1.** Key molecular orbitals of $SO_2$.

experimental values whereas the bond angles deviate by up to 4°.

We shall now turn to an explanation of why $E(NMe)_2$ (E = S, Se, Te) favor the more congested *syn,syn* (**1**) and *syn, anti* (**2**) conformations over *anti,anti* (**3**) with a minimal steric repulsion between the two NMe fragments. To this end, the electronic structures of $E(NMe)_2$ (E = S, Se, Te) will be discussed.

**Orbital Interactions in *N,N′*-Dimethylchalcogen Diimides.** In order to develop a qualitative understanding of the conformational preferences in $E(NMe)_2$ (E = S, Se, Te), it is helpful to consider first the isoelectronic molecule sulfur dioxide. The well-known molecular orbitals (MOs) of $SO_2$ are constructed from one s and three p atomic orbitals (AOs) on each nucleus.[32] Figure 1 shows the six occupied MOs of highest energy and the lowest unoccupied MO.

The corresponding MOs for $S(NMe)_2$ can be constructed by observing that the fragment NMe is isolobal with the oxygen atom. To a first approximation, two of the NMe fragment orbitals (**4a**, **4b**) are essentially the same as those of oxygen in

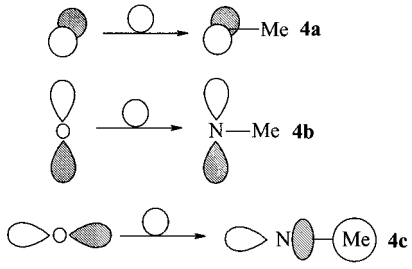


that they have approximate inversion symmetry at the nitrogen center. Thus, to a first approximation, the orbital energies for $1b_1$, $1a_2$, and $2b_1$ (Figure 1) will not differ in the three conformations of $S(NMe)_2$ as **4a** and **4b** of oxygen are replaced with the corresponding orbitals on the NMe fragment. On the other hand, the third NMe orbital, **4c**, is significantly different from that of oxygen because it lacks an inversion center at the nitrogen atom. Consequently, the orbital energies of $3a_1$, $3b_2$, and $4a_1$ will differ in the three conformations of $S(NMe)_2$ as **4c** of oxygen is replaced by the NMe analogue. The difference is particularly important for the bonding $3a_1$ orbital and its antibonding $4a_1$ counterpart, whereas the nonbonding orbital $3b_2$

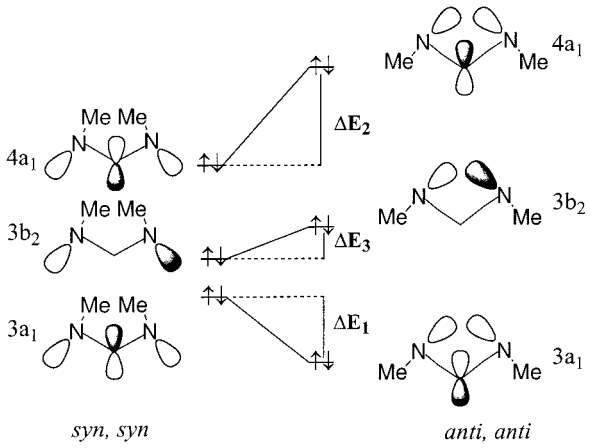


**Figure 2.** Correlation diagram for the $3a_1$ and $4a_1$ orbitals of the *syn,syn* and *anti,anti* isomers of $S(NMe)_2$.

obviously will be less influenced by the choice of conformation. This is illustrated in Figure 2 where the $3a_1$, $4a_1$, and $3b_2$ orbitals of $S(NMe)_2$ for the *syn,syn* and *anti,anti* conformations are shown. On the basis of geometrical considerations, the bonding $3a_1$ orbital is more stabilized and the antibonding orbital $4a_1$ more destabilized in the *anti,anti* compared to the *syn,syn* conformation. However, for the same in-phase, $3a_1$, and out-of-phase, $4a_1$, interactions, the destabilization energy, $\Delta E_2$, is numerically larger than the stabilization energy, $\Delta E_1$ (see Figure 2), consistent with standard perturbational molecular orbital (PMO) considerations. The orbital $3b_2$ is also destabilized to a lesser degree ($\Delta E_3$).

The qualitative PMO considerations given above can be used to rationalize why the *syn,syn* conformation is calculated to be more stable than the *anti,anti* isomer by our more quantitative DFT treatment for the entire series $E(NMe)_2$ (E = S, Se, Te), although the *syn,syn* conformation is sterically less favorable. The *syn, anti* isomer represents a compromise between optimal steric and electronic interactions. We find it to be very similar in energy to the *syn,syn* conformation (Table 1).

**Dimerization of *N,N′*-Dimethylchalcogen Diimides. (a) Calculated Structures and Energy of the Dimerization Reaction.** Sulfur diimides are thermally stable and have been structurally characterized with a variety of groups attached to the nitrogens,[6−12] whereas selenium diimides are thermally unstable at room temperature.[18] Tellurium diimides, on the other hand, do not exist as monomers; instead, the two known examples are thermally stable dimers.[19] In the solid state, $^t$-$BuNTe(\mu\text{-}N^tBu)_2N^tBu$ (**5**) adopts a *cis* structure (with respect to terminal $N^tBu$ groups), and in solution, no exchange between bridging and terminal $N^tBu$ groups is observed.[19b,c]

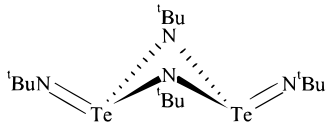


**5**

The calculated structure for the tellurium diimide dimers $RN{=}E(\mu\text{-}NR)_2E{=}NR$ (see Figure 3) was optimized with the *cis* butterfly shape and $C_{2v}$ symmetry. In Table 3, the calculated structural data are given, along with the data from the crystallographically characterized structure for the Te derivative with R = $^t$Bu. The calculated structure for the model tellurium dimer

(32) Gimarc, B. M. *Molecular Structure and Bonding: The Qualitative Molecular Orbital Approach*; Academic Press: New York, 1979.

(33) Ziegler, T.; Rauk, A. *Theor. Chim. Acta* **1977**, *46*, 1.

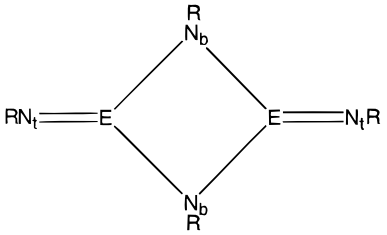


**Figure 3.** Schematic drawing of the dimer RN═E($\mu$-NR)$_2$E═NR.

**Table 3.** Comparison of the Optimized Structures for RN═E($\mu$-NR)$_2$E═NR (E = S, Se, Te; R = Me) with the X-ray Structure for E = Te and R = $^t$Bu

| | optimized structure | | | |
|---|---|---|---|---|
| bond lengths (Å)/ bond angles (deg)[a] | E = S; R = Me | E = Se; R = Me | E = Te; R = Me | X-ray structure[b] E = Te; R = $^t$Bu |
| $\|d(E-N_b)\|$ | 1.797 | 1.987 | 2.140 | 2.081(8) |
| $d(E=N_t)$ | 1.547 | 1.735 | 1.961 | 1.876(10) |
| $\angle(N_bEN_b)$ | 78.2 | 76.3 | 72.8 | 75.6(4) |
| $\|\angle(N_tEN_b)\|$ | 112.4 | 108.1 | 105.3 | 113.4(5) |
| $\|\angle(EN_bN)\|$ | 98.4 | 98.5 | 104.5 | 101.1(6) |

[a] The subscripts b and t refer to bridging and terminal nitrogen atoms, respectively. [b] Experimental data from ref 19b.

**Scheme 1**

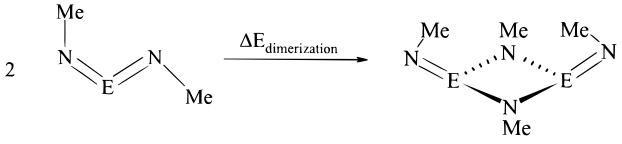


agrees fairly well with experiment, but the tellurium−nitrogen bond lengths are overestimated by 0.06−0.08 Å. Although the sulfur and selenium analogues of the dimer are unknown, similar *cis* butterfly structures were optimized with $C_{2v}$ symmetry. Comparison of Tables 2 and 3 shows that the exocyclic chalcogen−nitrogen bonds (E═N$_t$) are very slightly shorter than the chalcogen−nitrogen bonds in the monomeric chalcogen diimides, whereas the endocyclic bonds, as expected, are significantly longer. For example, the sulfur−nitrogen bond in the *syn*,*syn* isomer is 1.567 Å, while in the sulfur diimide dimer $d$(S═N$_t$) is 0.020 Å shorter. For the selenium and tellurium dimers, the exocyclic bond distances $d$(E═N$_t$) are 0.044 and 0.030 Å shorter, respectively, compared to the value of $d$(E═N) for the lowest energy *syn, anti* isomers. The changes to the endocyclic E−N$_b$ bonds are more significant for the lighter chalcogens; down the group from sulfur to tellurium, the increases are 0.230, 0.208, and 0.149 Å, respectively.

To determine the energy of the hypothetical dimerization process (Scheme 1), the model system MeN═E($\mu$-NMe)$_2$E═NMe was optimized for E = S, Se, Te. Using the generalized transition state method,[33] the steric and electronic contributions to the dimerization energy can be separated:

$$\Delta E_{\text{dimerization}} = E(\text{dimer}) - 2E(\text{monomer}) \qquad (1)$$

according to

$$\Delta E_{\text{dimerization}} = [2\Delta E_{\text{prep}} + (\Delta E^\circ + \Delta E_{\text{el}})] \qquad (2)$$

$\Delta E_{\text{prep}}$ is the energy required to alter the geometry of the planar monomer to its geometry as a distorted fragment of the dimer. We shall discuss this distortion below. The term $\Delta E^\circ$ represents the energy of steric interaction between monomers. It includes the stabilizing electrostatic interaction between the two fragments and the exchange repulsion component resulting from the destabilizing interactions between occupied orbitals on each fragment. Finally, $\Delta E_{\text{el}}$ of eq 2 accounts for the stabilizing interactions between occupied and empty fragment orbitals. The quantity ($\Delta E^\circ + \Delta E_{\text{el}}$) represents the energy gained by coupling the distorted fragments.

**Table 4.** Calculated Energies for Dimerization of E(NMe)$_2$ (E = S, Se, Te)[a]

| E | $\Delta E_{\text{prep}}$ | $\Delta E^\circ + \Delta E_{\text{el}}$ | $\Delta E_{\text{dimerization}}$[b,c] |
|---|---|---|---|
| S | 190.9 | −346.9 | 34.9 |
| Se | 144.8 | −292.4 | −2.8 |
| Te | 125.3 | −333.3 | −82.9 |

[a] kJ mol$^{-1}$. [b] $\Delta E_{\text{dimerization}} = 2\Delta E_{\text{prep}} + (\Delta E^\circ + \Delta E_{\text{el}})$. [c] See text for definition of $\Delta E_{\text{prep}}$, $\Delta E^\circ$, and $\Delta E_{\text{el}}$.

The observed experimental state (monomer or dimer) of the chalcogen diimides is dependent on the energetics of the dimerization reaction (Table 4). The coupling of the distorted diimide fragments ($\Delta E^\circ + \Delta E_{\text{el}}$) is energetically favorable for all three chalcogens. However, the preparation energy of 190.9 kJ mol$^{-1}$ for the sulfur diimide is much larger than that for the tellurium analogue (125.3 kJ mol$^{-1}$). This difference is factored into the energy of dimerization twice (since two monomers are required to make a dimer), and this costs more energy (381.8 kJ mol$^{-1}$) than is gained by the orbital interactions (−346.9 kJ mol$^{-1}$); therefore, the reaction is considerably endothermic ($\Delta E_{\text{dimerization}}$ = 34.9 kJ mol$^{-1}$). This is consistent with the experimental observation of monomeric sulfur diimides. For *N*,*N*′-dimethylselenium diimide, the dimerization is not significantly exothermic ($\Delta E_{\text{dimerization}}$ = −2.8 kJ mol$^{-1}$). Experimentally, selenium diimides appear to be monomers that decompose quickly.[18] On the other hand, the dimerization is clearly exothermic for *N*,*N*′-dimethyltellurium diimide ($\Delta E_{\text{dimerization}}$ = −82.9 kJ mol$^{-1}$), which has the smallest preparation

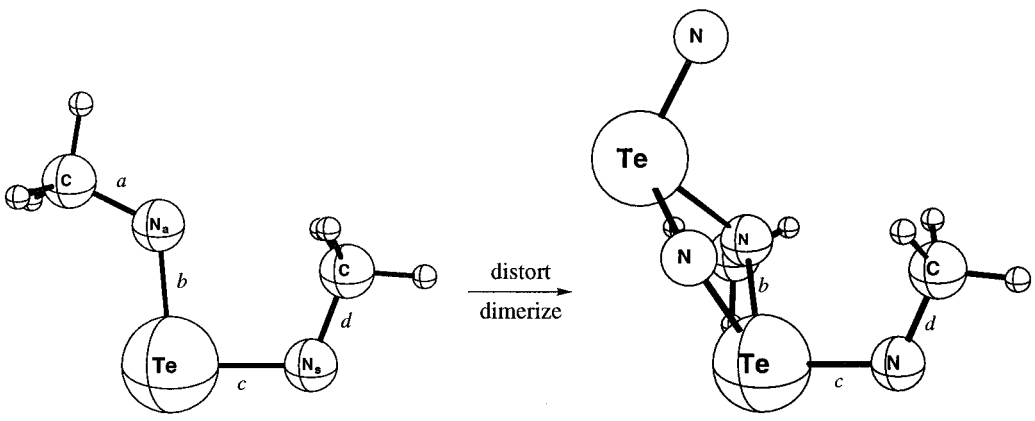


**Figure 4.** Distortion of planar tellurium diimide to fragment geometry.

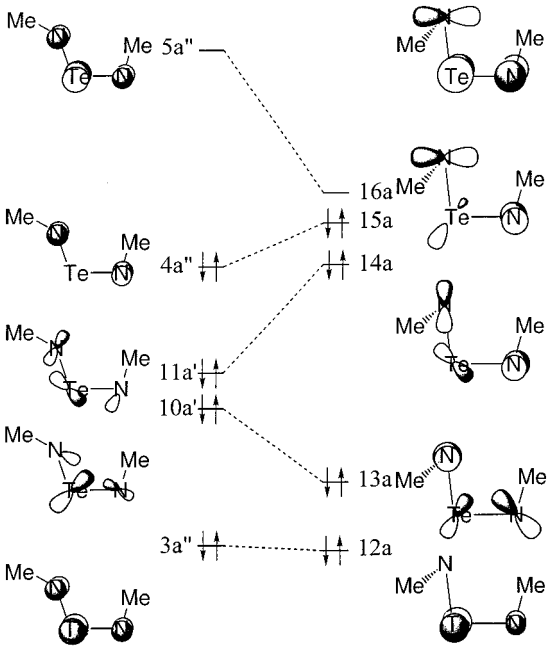


**Figure 5.** Distortion of planar tellurium diimide MOs to MOs with fragment geometry. Contributions from the orbitals of methyl groups have been omitted for clarity.

energy ($\Delta E_{prep}$ = 125.3 kJ mol$^{-1}$), in agreement with the observed dimeric nature of tellurium diimides.[19]

The trend in preparation energies correlates with predicted chalcogen−nitrogen double-bond energies; it is more difficult to stretch a sulfur−nitrogen bond with a large 3p−2p overlap than to elongate a tellurium−nitrogen bond with a more modest 5p−2p overlap. The difference in preparation energies is also revealed in the changes to bond lengths mentioned above. The most pronounced lengthening of 0.230 Å in the endocyclic sulfur−nitrogen bond of the dimer corresponds to the largest preparation energy of 190.9 kJ mol$^{-1}$. We shall now turn to a more detailed analysis of the orbital interactions involved in the dimerization of *N,N′*-dimethylchalcogen diimides.

**(b) Orbital Interactions in the Dimerization of *N,N′*-Dimethyltellurium Diimide.** The lowest energy geometry of *N,N′*-dimethyltellurium diimide is the *syn,anti* isomer. To "prepare" this monomer for dimerization, the geometry must be distorted. Figure 4 shows the changes to bond lengths and angles that occur in the distortion from monomer to the fragment

**Table 5.** Orbital Populations of Fragment Orbitals

| orbital | population (e) in monomer | population (e) in dimer | change |
|---|---|---|---|
| 13a | 2.0 | 1.87 | −0.13 |
| 14a (HOMO-1) | 2.0 | 1.58 | −0.42 |
| 15a (HOMO) | 2.0 | 1.53 | −0.47 |
| 16a (LUMO) | 0.0 | 0.98 | +0.98 |

geometry. The bonds *a, b,* and *d* stretch while bond *c* contracts slightly. The bond angles *ab* and *cd* close, and bond angle *bc* opens up. The dihedral distortions from the planar monomer correspond to *abc* changing from 180 to 38° and to *bcd* changing from 0 to 96°. The *anti* NMe becomes the bridging NMe in the dimer, as can be seen in Figure 4, where the NTe skeleton from the second fragment in the dimer is shown.

The orbitals of the *syn, anti* isomer are distorted into the fragment orbitals as shown in Figure 5. The almost 90° twist of *abc* will move the out-of-plane p contribution on the endocyclic nitrogen. This is shown for the LUMO and the four highest occupied orbitals. This distortion lowers the energy of the LUMO, while raising the energy of the two other most important orbitals for the dimerization process. The distorted fragment does not have the same symmetry requirements as the planar monomer; therefore, the fragment orbitals will mix. For example, this can be seen in the changes to the HOMO. Because the fragment is not planar, symmetry does not require only out-of-plane p contributions for the tellurium and exocyclic nitrogen. Also, in the planar HOMO, there is no contribution from tellurium because none of its AOs can effectively overlap with the out-of-phase out-of-plane nitrogen lone pairs. The distorted fragment does not have this restriction, and a contribution from tellurium mixes in as shown in Figure 5.

When the fragment molecular orbitals of the monomers combine to form the molecular orbitals of the dimer, the fragment orbital populations change. Table 5 gives the most important populations. In the bonding that holds the dimer together, the three highest MOs on each monomer are depopulated while the LUMO of each monomer is populated. The contributions of these monomer fragment orbitals to the dimer molecular orbitals are most significant in the frontier orbitals of the dimer as described below.

The bonding interactions between fragment orbitals are depicted in Figure 6 and are viewed along the $C_2$ axis in the direction shown. The two fragments join along the dashed lines in the $Te_2N_2$ ring. On the basis of the occupations of the

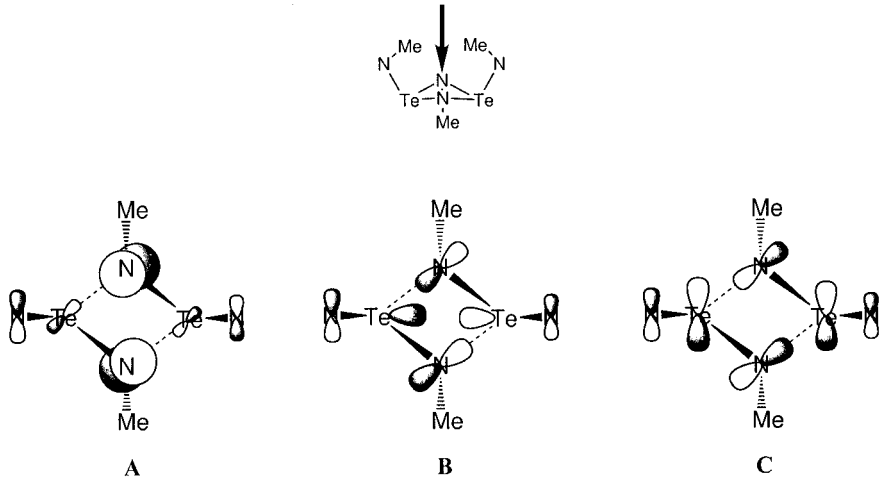


**Figure 6.** Important orbital interactions in the dimerization process: (A) (HOMO-1)−(HOMO-1); (B) HOMO−HOMO; (C) LUMO−LUMO. Methyl groups attached to terminal N atoms are omitted for clarity.

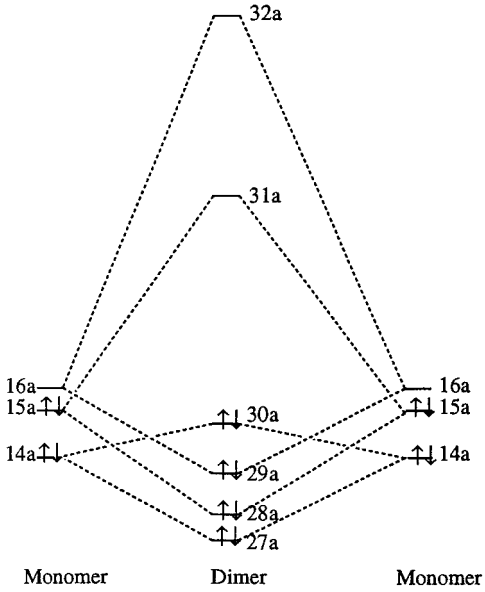


**Figure 7.** Key molecular orbitals for the dimerization process.

fragment orbitals, one might expect the (HOMO-1)s and the HOMOs of the fragments to combine as four-electron destabilizing interactions. The actual orbital energies in Figure 7 show that this is not in fact the case. The destabilized antibonding HOMO−HOMO combination rises in energy to become the LUMO of the dimer. The electrons instead occupy the bonding LUMO−LUMO combination, which is more stabilized than the antibonding HOMO−HOMO. The dashed lines in Figure 7 show the most significant contributions of fragment orbitals to the dimer orbitals. All orbitals have A symmetry and can mix with these frontier orbitals, so the fragment HOMO is not the only depopulated orbital. As mentioned above, the three highest occupied orbitals on each fragment lose electrons to the fragment LUMO.

## Conclusions

DFT calculations indicate that the *syn*,*syn* and *syn*, *anti* isomers of the chalcogen diimides $E(NMe)_2$ have very similar relative energies for all three chalcogens whereas the *anti*,*anti* isomers are considerably higher in energy. The calculated energies for the dimerization of these monomers reveal that this process is endothermic for E = S, thermochemically neutral for E = Se, and strongly exothermic for E = Te, consistent with the experimental observation of dimeric structures for tellurium diimides. An analysis of the contributions to the dimerization energies reveals that these differences can be attributed to the expected trend to lower $\pi$-bond energies for chalcogen−nitrogen ($n$p−2p)$\pi$-bonds along the series S($n$ = 3), Se($n$ = 4), Te($n$ = 5). Examination of the orbital interactions involved provides considerable qualitative insight into the nature of the dimerization process. In essence, the three highest occupied orbitals on each monomer are depopulated and a bonding combination of the monomer LUMOs is populated to provide the bridge bonding in the dimer. These calculations suggest that dimeric chalcogen diimides involving two different chalcogens, e.g. Se/Te or, perhaps, S/Te, may be stable. Attempts to prepare such dimers are in progress.

**Acknowledgment.** We thank the NSERC (Canada) for financial support.

IC970680F